Phases in strongly coupled electronic bilayer liquids

V. I. Valtchinov,[1,2] G. Kalman,[1] and K. B. Blagoev[1]
[1]*Department of Physics, Boston College, Chestnut Hill, Massachusetts 02167*
[2]*Department of Radiology, Brigham and Women's Hospital, Harvard Medical School, Boston, Massachusetts 02115*
(Received 24 December 1996)

The strongly correlated liquid state of a bilayer of charged particles has been studied via the hypernetted chain calculation of the two-body functions. We report the first time emergence of a series of structural phases, identified through the behavior of the two-body functions. [S1063-651X(97)10609-2]

PACS number(s): 64.70.Ja, 71.45.−d, 73.61.−r, 64.90.+b

Electronic bilayer systems, consisting of two quasi-two-dimensional layers of electron (or hole) liquids, separated by a distance d comparable to the interparticle separation a (the Wigner-Seitz radius) within the layers, have revealed an unexpected richness of features, and have been the object of many recent investigations. While most of the interest has originated from the quantum Hall effect, and thus the related studies have been directed at bilayers in strong magnetic fields, more recently it has been recognized that unmagnetized bilayers also constitute a physical system of remarkable complexity. Electronic bilayer systems in semiconductors can now be quite routinely fabricated by modern nanotechnology in a fairly wide range of densities (i.e., r_s values) and interlayer separations. Interestingly, virtually similar systems have also come into existence under quite different circumstances in ionic traps, where the charged particles are classical ions and the layers develop as a result of the system seeking its minimum-energy configuration [1–3].

At high enough r_s ($=a/a_B$, $a_B=\varepsilon_b\hbar^2/m^*e^2$ is the effective Bohr radius) or Γ ($=e^2/akT$) values (estimated to be between $\Gamma=98$ and $\Gamma=222$ [4]) a classical bilayer is expected to crystallize into a Wigner lattice. While there is no direct experimental evidence or the formation of such an electronic solid in semiconductor bilayers without magnetic field (since the required $r_s\simeq 37$ values do not seem to be attainable by present-day experimental technique), the formation of layered crystalline structures has been observed in molecular-dynamics computer simulations [2] and in ionic traps [3]. At the same time, a series of rather thorough theoretical investigations [1,4–6] have been carried out predicting the formation of classical Wigner lattices in electronic or ionic bilayers. These studies have revealed the existence of distinct structural phases, whose characteristics depend on the layer separation, i.e., on the d/a ratio (see the inset in Fig. 2): the staggered rectangular (ii), the staggered rhombic (iv), and the staggered triangular (v). Structure (ii) comprises the simple triangular (i) and the staggered square (iii), as special cases. A similar quantum-mechanical study for the magnetized bilayer [7] has led to very similar predictions.

The understanding of the experimentally more important (and theoretically perhaps more challenging) *liquid phase*, on the other hand, is quite incomplete. Its analysis hinges upon the availability of the *intralayer* and *interlayer* two-body functions [$g_{11}(r)$ and $g_{12}(r)$, respectively]. While attempts have been made to determine the g_{ij}'s through various approximations, none of the results obtained can be considered reliable, especially with regard to the developing short-range order: Zheng and McDonald [8] and Neilson and co-workers [9], used the Singwi-Tosi-Land-Sjolander approach, whose limitations are well known; Kalman, Ren, and Golden [10] used a quasi-iterative method, which breaks down for small layer separations.

The purpose of this paper is to provide a summary of the first reliable calculation of the pair correlation functions $g_{ij}(r)$ and related quantities such as the structure functions $S_{ij}(k)$ and the dielectric matrix $\varepsilon_{ij}(k)$ for a bilayer system. The results show that different short-range ordered structures develop in the liquid phase, at relatively modest coupling values, emulating the different structural phases in the Wigner lattices. The gradual increase of the layer separation is accompanied by dramatic changes in $g_{ij}(r)$, $S_{ij}(k)$, and $\varepsilon_{ij}(k)$ that can be partially interpreted in terms of the structural changes referred to above, partially in terms of a new type of *substitutional* orded-disorder transition. The bilayer turns out to be a unique liquid system exhibiting structural transformations of the phase pursuant to the change of a system parameter: such transformations are commonly known only in the *solid* phase.

Our method of approach is based on the classical HNC (hypernetted chain) approximation. This method has proven to be extremely reliable and accurate for Coulomb systems, both in three [11,12] and two dimensions [13–15]. We adapted the HNC method to the bilayer situation, by mapping the (single component) bilayer onto a two-component two-dimensional (2D) system, with an interaction potential matrix [15,16]

$$\varphi_{11}=\varphi_{22}=\frac{2\pi e^2}{r}, \quad \varphi_{12}=\varphi_{21}=\frac{2\pi e^2}{\sqrt{r^2+d^2}}; \tag{1}$$

and using the two-component equivalent of the HNC method. The two layers are assumed to have equal densities n. The resulting system of equations for $g_{ij}(r)=h_{ij}(r)+1$, $c_{ij}(r)$, and their Fourier transforms $h_{ij}(k)$ and $c_{ij}(k)$,

$$h_{ij}(r)=e^{h_{ij}(r)-c_{ij}(r)-\phi_{ij}(r)}-1,$$

$$h_{12}(k)=\frac{c_{12}(k)}{[1-nc_{11}(k)]^2-[nc_{12}(k)]^2}, \tag{2}$$

$$h_{11}(k)=\frac{c_{11}(k)+nc_{12}(k)h_{12}(k)}{1-nc_{11}(k)},$$

has been solved following Lado's original work on 2D sys-

tems [15]. The underlying model is a classical one, where the average kinetic energy is represented by the inverse temperature parameter β and the intralayer coupling by the parameter $\Gamma = e^2/akT$. This description is appropriate for bilayers arising in ionic traps if the confining potential is steep enough so that the degree of freedom perpendicular to the bilayer planes is suppressed; it is also expected to be quite adequate for the analysis of the spin-independent structural phases of the zero-temperature electron liquid, in the domain of high enough coupling ($a > a_B$) where the electrons are quasilocalized and the effect of intralayer exchange becomes small. Interlayer tunneling effects also disappear under the usually less stringent $d > a_B$ condition. Under these circumstances, invoking the equivalence $\Gamma \simeq 2r_s$ is a reasonable prescription for the interpretation of the results derived from the present model of semiconductor bilayers.

Our result for the intralayer $g_{11}(r)$ and interlayer $g_{12}(r)$ two-body functions are summarized in Fig. 1 which shows their variation as functions of the coupling Γ and of the interlayer separation d/a. In order to quantitatively analyze the information contained in the results we have used as principal indicators the following quantities:

(i) $g_{12}(0)$, the measure of the probability of finding a particle in layer 2 above another particle in layer 1: when the interlayer correlations become significant, $g_{12}(r)$ approaches zero.

(ii) R_I, R_{II}, R_{III} and Q_I, Q_{II}, Q_{III}, the positions of the first three maxima of $g_{11}(r)$ and $g_{12}(r)$, respectively: these maxima identify the correlation shells around a given particle, both in its own layer and in the layer adjacent to it.

(iii) The intralayer coordination numbers ρ_I, ρ_{II}, ρ_{III} and the interlayer coordination numbers σ_I, σ_{II}, σ_{III}, associated with each shell; the coordination numbers are defined by

$$\rho_i = 2n\pi \int_{M_i'}^{M_i''} r g_{11}(r) dr, \quad \sigma_i = 2n\pi \int_{N_i'}^{N_i''} r g_{12}(r) dr,$$

where M_i' (N_i') and $M_i''(N_i'')$ are the minima preceding and following $R_i(Q_i)$.

Short-range order, signaled by the onset of oscillating behavior for $g_{11}(r)$ appears around $\Gamma_s = 3$, more or less the same value as for the isolated 2D layer. The value of Γ_s does not seem to be significantly affected by the layer separation d. Once the short-range order has developed, the most dramatic feature of the two-body functions is the series of quite abrupt shifts in the positions and changes in the amplitudes of the first few peaks both of $g_{11}(r)$ and of $g_{12}(r)$. This can be well observed in Figs. 1 and 2. These features unambiguously point at the formation and phase-transformation-like changes of short-range structures in the bilayer electron liquid, which can be paralleled with the results of recent studies of the bilayer crystalline phase [1,4–6].

The physical features of the system are revealed through the two-body functions, the structure functions and the dielectric matrix of the system. In order to bring out the characteristic features in the details of the structure of two-body functions, we used the rather high $\Gamma = 80$ value for the latter. For the structure functions and for the dielectric matrix we used the more realistic $\Gamma = 20$ and $\Gamma = 10$ values.

(1) *Two-body functions* $g_{11}(r)$, $g_{12}(r)$.

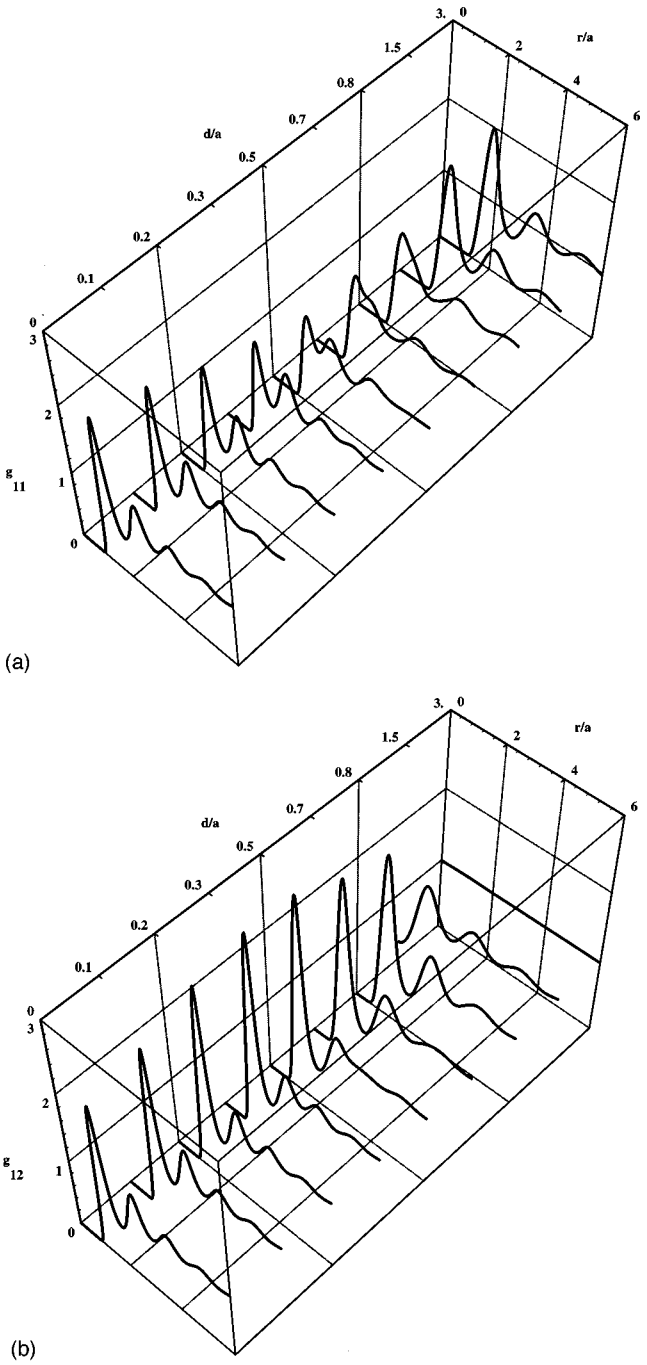

FIG. 1. Variation of the structure of the two-body functions with increasing layer separations d/a at $\Gamma = 80$: (a) $g_{11}(r)$; (b) $g_{12}(r)$.

(1.1) Interlayer correlations, as inferred from $g_{11}(0)$, seem to completely disappear for about $d/a = 3$, even for very high Γ values (see the inset of Fig. 2). Thus for layer separations higher than this value the two layers behave as virtually independent 2D systems.

(1.2) The positions, heights, widths, and resulting coordination numbers of the correlation shells shift and change drastically as the interlayer separation is increased (see Fig. 2). These changes can be brought into correspondence with the expected formation of the different lattice structures in the solid phase, as discussed above. Since each lattice structure carries a precise set of nearest neighbor positions $\{R_\alpha\}$, $\{Q_\alpha\}$ and coordination number $\{\rho_\alpha\}$, $\{\sigma_\alpha\}$ (with α

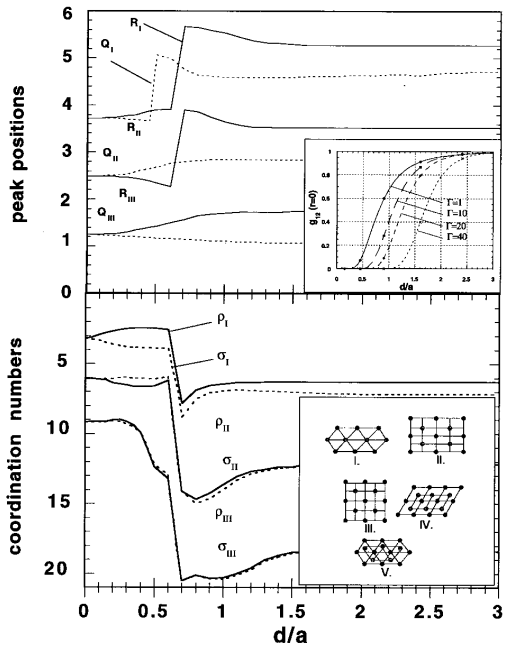

FIG. 2. Characteristic variation with layer separation of the first, second, and third maxima of $g_{11}(r)$ and $g_{12}(r)$: (a) positions R_I, R_{II} (b) associated coordination numbers ρ_{II}, ρ_{II}, ρ_{III} and σ_I, σ_{II}, σ_{III}. The insets show the five principle lattice structures and the value $g_{12}(r)$ at $r=0$.

$=1,2,3,\ldots$ representing the first, second, third, etc. nearest neighbors in the lattice), these can be identified with the previously defined $\{R_i\}$, $\{Q_i\}$, $\{\rho_i\}$, and $\{\sigma_i\}$ (values with $i=I$, II, and III, representing the first, second and third shell positions). (The identification is not one to one: a given shell, in general, with the possible exception of the first shell, contains more than one set of nearest neighbors). Thus the formation of a series of ''liquid phases'' emulating the underlying lattice structural phases can be observed.

(1.3) At $d=0$, when the two layers are collapsed into a single 2D system with double density $2n$, their two two-body functions $g_{11}(r)$ and $g_{12}(r)$ are identical, with $R_{II}/R_I = Q_{II}/Q_I \simeq 1.9$ ratio, slightly higher than the characteristic $\sqrt{3}$ of a triangular lattice. The $R_I=Q_I=1.25$ value itself is somewhat below the lattice constant $R_1=1.34$, similarly to what has been obtained in the Monte Carlo and HNC [13–15] calculations for an isolated 2D electron liquid. The double-density triangular structure can also be regarded as a staggered rectangular lattice with a side ratio $a_2/a_1=\sqrt{3}$. The identity of the two two-body functions g_{11} and g_{12} and the accompanying equality of the coordination numbers, $\rho_i=\sigma_i$, however, clearly indicates that the two species are in a complete *substitutional disorder*, occupying the lattice sites at random. Should this not be the case, the two functions $g_{11}(r)$ and $g_{12}(r)$ would remain distinct even for very small $(d\rightarrow 0)$ layer separation.

(1.4) With d increasing away from the zero value, the substitutional *disorder* is rapidly replaced by a substitutional *order* appropriate for the staggered rectangular structure: by $d/a=0.5$, ρ_I and σ_I assume their expected $\rho_1=2$ and $\sigma_1=4$ values. At the same time, the rectangular unit cell deforms toward a squarelike shape: this is well shown by the reduction of R_{II}/R_I to the $\simeq 1.5$ value. The substitutional disorder that prevails in the domain $0<d/a<0.5$ would seem to require that vestiges of the peaks of $g_{11}(r)$ show up in $g_{12}(r)$ and vice versa. This, however, is apparently *not* the case: R_I and Q_I, R_{II} and Q_{II}, etc., are quite distinct. Nevertheless, the separations between R_i and Q_i remain small enough and the peaks wide enough to accommodate the substitutionally ill-positioned particles. In fact, the Q_{III} shell appears to be thriving on the ill-positioned population: by the establishment of the substitutional order the II shell at $Q_{II}=3.65$ vanishes, and is replaced by the more distant position at $Q_{III}=4.99$.

(1.5) The transformation to an underlying staggered square lattice structure becomes complete at $d/a=0.7$. The indicators of this transformation are the jump of R_{II} from 2.30 to 3.89 and R_{II} from 3.87 to 5.63, and the accompanying jump of the coordination numbers ρ_I from $\simeq 2$ (the same as ρ_1 for the rectangular lattice) to $\simeq 7$ [close to $\rho_1+\rho_2=8$ $(\rho_1=4,\ \rho_2=4)$ for the square lattice]. All these changes reflect the higher symmetry of the square lattice.

(1.6) In the domain $d/a>0.7$ the staggered square lattice gradually transforms into a staggered *rhombic* lattice with $90>\varphi>60°$: this allows an energetically favorable increase of the lattice constant, at the cost of a *decrease* of the energetically less important second and third neighbors. This trend is very clearly observable in the behavior of R_I, R_{II}, and R_{III}, and also detectable in Q_I and Q_{III}. There is no significant change in the coordination numbers in this domain, except a slight reduction in ρ_I, ρ_{II}, σ_I, and σ_{II} reflecting the reduced distance between the corresponding shells.

(1.7) Around $d/a=1.6$, φ reaches the 60° value, and in each layer the underlying structure becomes a standard 2D triangular (hexagonal) lattice, with a lattice constant appropriate for density n. This can be inferred from R_I reaching its maximum and R_{II}, R_{III} and Q_I, Q_{II}, Q_{III} reaching their minimum values, the former very close to $\sqrt{2}$ times the $R_I(d=0)$, $R_{II}(d=0)$, and $R_{III}(d=0)$ values, respectively.

(1.8) The triangular lattices emerging as the end product of the rhombic structure are staggered in such a way that the vertices of layer 2 lie over the midpoints of the sides of the triangles in layer 1 (and vice versa). This is not the minimum-energy configuration for well-separated layers: this latter is attained when the vertices of the 2-triangles lie over the centers of the 1-triangles. Transition to this final configuration, consisting of a rigid translation of lattice 2 with respect to lattice 1, takes place in the domain $(1.5)<d/a\simeq 2.0$ and is shown by a slight, but perceptible increase in Q_I and Q_{III}.

(2) *Structure functions* $S_{11}(k)$, $S_{12}(k)$ (Fig. 3). The expected small-k behavior of the structure function is governed by a generalized compressibility sum rule [17]: at $k=0$ the $S_{11}(0)=-S_{12}(0)$ condition is required; both of the values of $S_{11}(0)$ and of $[\partial S_{11}(k)/\partial k]$ $(k=0)$ are governed by the quantity $L_{11}-L_{12}$, the difference between the inverse compressibility and the inverse trans-compressibility $L_{ij}=(\partial P_i/\partial A_j)K_o$, where K_o, P and A are respectively the compressibility of the noninteracting gas, the pressure, and the surface area (for the observability of these quantities, see Ref. [18]). At $d=0$ the purely correlational L_{12} compensates

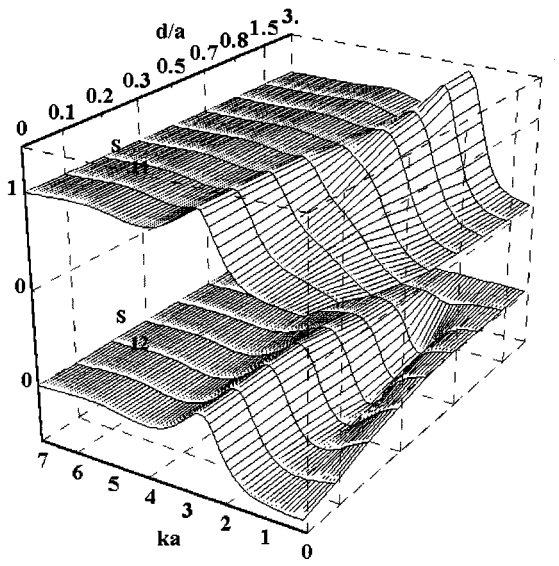

FIG. 3. Variation of the structure functions with increasing layer separations d/a for $\Gamma=20$ for $S_{11}(k)$ and $S_{12}(k)$. Note that the coordinates of S_{11} and S_{12} are shifted with respect to each other.

for the correlational contribution to the L_{11} [resulting in $S_{11}(0)=-S_{12}(0)=1/2$]. This is also the consequence of the perfect screening sum rule which requires that $n\int d^2r\{h_{11}(r)+h_{12}(r)\}=-1$. For high-$d$ values, L_{11} becomes dominant, approaching the value appropriate for the isolated 2D layer, which, for $\Gamma\geqslant 1$ is $L_{11}=1-0.821\Gamma$ [19]. The inset in Fig. 2 shows the $L_{11}-L_{12}$ values, extracted from $S_{11}(k)$ and $S_{12}(k)$, corroborating the expected behavior.

(3) *Dielectric response matrix.* The inverse of the static dielectric response matrix $\eta(k)=\varepsilon^{-1}(k)$ can be expressed in terms of the structure functions as $\eta_{ij}(k)=\delta_{ij}-\beta n\varphi_{il}(k)S_{lj}(k)$. It determines the total potential Φ_i in the two layers when either of them is perturbed by an external potential $\hat{\Phi}_i$:

$$\Phi_i=\eta_{ij}\hat{\Phi}_j\,.$$

At small layer separation the effective dielectric function $\det\varepsilon_{ij}$ has the features of the dielectric function of an isolated 2D layer (see Fig. 4) with the characteristic antiscreening behavior for $k<k_*$ (~ 25). This behavior becomes qualitatively different precisely at the layer separation where $L_{11}-L_{12}$ changes from positive to negative (see the inset of Fig. 4) [17]: ε_{11} and ε_{12} develop alternatively anti-screening and screening domains.

We can compare our results concerning the critical values of d/a at the phase transition boundaries with those in the works of Goldoni and Peeters (GP) [4] into our d/a values. Table I shows the comparison. The d/a $[(ii)\rightarrow(iii)]$ value has been taken along the liquid-solid phase boundary at the lowest Γ value ($\Gamma=118$) in Fig. 8 [4(a)]. GP claimed a wide range of stability ($0.79<d/a<1.10$) for the staggered square lattices. We do not see this happening: the gradual transformation into a rhombic structure seems to follow immediately the formation of the square lattice. The expected first order character of the (iv)–(v) transition is masked in the present description. Neither is there a clear indication of the transition taking place at $\varphi=69.6°$ predicted by GP rather than at $\varphi=60°$ (the indicator would be a slight decrease in the ρ_i values accompanying the detectable slight increase in the Q_i values). The possibility of substitutional disorder is not part of the GP lattice model, which allows for structural changes only, although, as our analysis reveals, it would be, for a finite temperature, a determining factor of the phase structure of the system in the $d/a<0.5$ domain (cf. Ref. [20]).

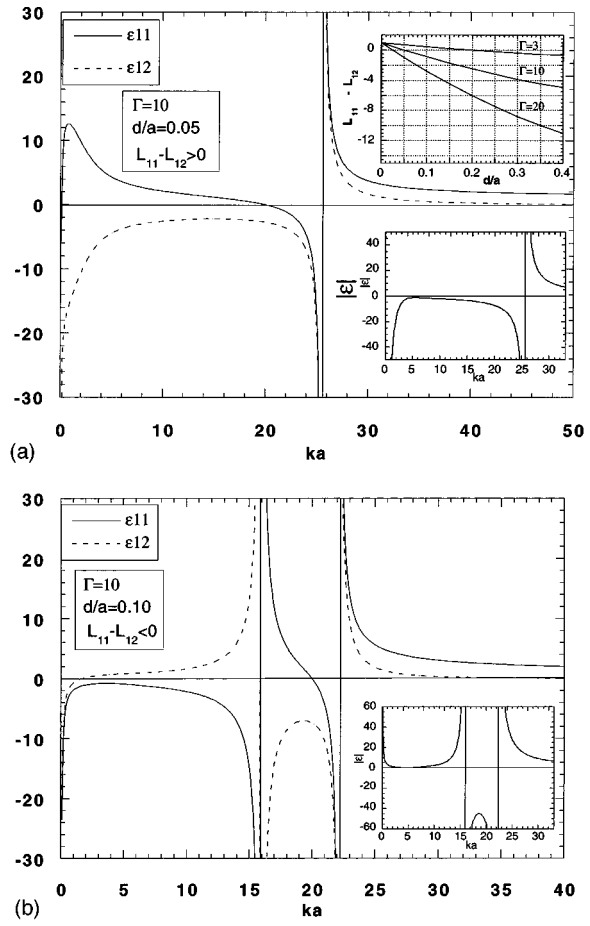

FIG. 4. Diagonal and off-diagonal elements of the static dielectric matrix for different layer separations (a) $d/a=0.05$ ($L_{11}>L_{12}$) and (b) $d/a=0.1$ ($L_{11}<L_{12}$) at $\Gamma=10$. The insets show $\det\varepsilon_{ij}$ and $L_{11}-L_{12}$, the difference between diagonal and trans inverse compressibilities.

TABLE I. Phase boundaries [(i): simple triangular; (ii/a): substitutionally disordered staggered quadrangular; (ii/b): substitutionally ordered staggered quadrangular; (iii): staggered square; (iv): staggered rhombic; (v): staggered triangular].

Phases	d/a This work	d/a GP (a)	d/a GP (c); $r_s\approx 30$	d/a GP (c); $r_s\approx 38$
(ii/a)→(ii/b)	~0.5			
(ii)→(iii)	0.7–0.8	0.79	0.57	0.50
(iv)→(v)	1.5–2.0	1.87	1.07	1.12

In summary, we have calculated the two-body functions, structure functions, and static dielectric matrix of a strongly correlated electronic bilayer liquid through the classical HNC approach. We have found a series of dramatic changes in the liquid structure as the layer separation varies from $d/a=0$ to $d/a=3$. These changes can be brought into correspondence with the structural transformations and with substitutional order-disorder transformations in the underlying lattice structure. This behavior seems to have been predicted [20] in other strongly correlated liquid systems. We have also shown how the structure functions and the static dielectric matrix reflect these structural changes.

This work was partially supported by NSF Grant No. PHY-9115714. Part of the work was done while G.K. was visiting at the University of California at San Diego, and he is grateful to Tom O'Neil for his hospitality. We would like to thank Dan Dubin for the discussions and for making his unpublished data available, and to Ken Golden of the University of Vermont for a series of useful conversations.

[1] D. H. E. Dubin, Phys. Rev. Lett. **66**, 2076 (1991); **71**, 2753 (1993); Phys. Fluids B **5**, 295 (1993).

[2] H. Totsuji and J.-L. Barrat, Phys. Rev. Lett. **60**, 2484 (1988); R. W. Hasse and J. P. Schiffer, Ann. Phys. (N.Y.) **203**, 419 (1990); A. Rahman and J. Schiffer, Phys. Rev. Lett. **57**, 1133 (1986); J. P. Schiffer, *ibid.* **71**, 818 (1993).

[3] S. L. Gilbert, J. J. Bollinger, and D. J. Wineland, Phys. Rev. Lett. **60**, 511 (1988); G. Birkl, S. Kassner, and H. Walther, Nature (London) **357**, 310 (1992); J. N. Tan, J. J. Bollinger, B. Jelencovic, W. M. Itano, and D. J. Wineland, in *Physics of Strongly Coupled Plasmas*, edited by W. D. Kraeft and M. Schlanges (World Scientific, Singapore, 1996), p. 387.

[4] (a) G. Goldoni and F. M. Peeters, Phys. Rev. B **53**, 4591 (1995); and (b) in *Proceedings of the 23rd International Conference on the Physics of Semiconductor Physics*, edited by M. Scheffer and R. Zimmermann (World Scientific, Singapore, 1996), Vol. 3; and (c) Europhys. Lett. **33**, 293 (1997).

[5] V. I. Falko, Phys. Rev. B **49**, 7774 (1994).

[6] K. Esfarjani and Y. Kawazoe, J. Phys.: Condens. Matter **7**, 7217 (1995).

[7] S. Narasimhan and T. L. Ho, Phys. Rev. B **62**, 12 291 (1995).

[8] L. Zheng and A. H. MacDonald, Phys. Rev. B **49**, 5522 (1994).

[9] L. Swierkowski, D. Neilson, and J. Szymanski, Aust. J. Phys. **46**, 423 (1993); D. Neilson, L. Swierkowski, J. Szymanski, and L. Liu, Phys. Rev. Lett. **71**, 4035 (1993); **72**, 2669 (1994).

[10] G. Kalman, Y. Ren, and K. I. Golden, in *Proceedings of the VI Workshop on the Physics of Nonideal Plasmas*, edited by T. Bornath and W. D. Kraeft [Contrib. Plasma Phys. **33**, 449 (1993)].

[11] G. S. Stringfellow, H. DeWitt, and W. Slattery, Phys. Rev. A **41**, 1105 (1989).

[12] F. J. Rogers, D. A. Young, H. E. DeWitt, and M. Ross, Phys. Rev. A **28**, 2990 (1983).

[13] H. Totsuji, Phys. Rev. A **17**, 399 (1978).

[14] R. C. Gann, S. Chakravarty, and G. V. Chester, Phys. Rev. B **20**, 326 (1979).

[15] F. Lado, Phys. Rev. B **17**, 2827 (1978).

[16] V. I. Valtchinov, G. Kalman, and K. B. Blagoev, in *Physics of Strongly Coupled Plasmas* (Ref. [3]), p. 139.

[17] G. Kalman and K. I. Golden (unpublished).

[18] I. S. Millered *et al.*, Appl. Phys. Lett. **68**, 3323 (1996).

[19] K. I. Golden, G. Kalman, and Ph. Wyns, Phys. Rev. A **61**, 6940 (1990).

[20] A. C. Mitus and A. Z. Patashinskii, Phys. Lett. **87A**, 179 (1982).